ORIGINAL PAPER

Experimental and theoretical investigations of spectroscopic properties of azobenzene derivatives in solution

**Robert Zaleśny · Katarzyna Matczyszyn ·
Anna Kaczmarek · Wojciech Bartkowiak ·
Piotr Cysewski**

Abstract The UV-Vis spectra of series of polymethyl-methacrylate (PMMA) copolymers with attached trans-azobenzene derivatives were measured in 1,1,2-trichloroethane. In order to gain some insight into the recorded spectra, the quantum chemical calculations were performed for the substituted azobenzenes using both configuration interaction with single excitations method (CIS) as well as density functional theory (DFT) with B3LYP and PBE0 functionals. The calculations were performed in solvent. In particular, we found that the PBE0 excitation energies are in very good agreement with the experimental data.

Keywords Photoisomerization · Azobenzene derivatives · UV/Vis spectra · Excitation energies · Density-functional theory

R. Zaleśny (✉) · P. Cysewski
Department of Physical Chemistry, Collegium Medicum,
Nicolaus Copernicus University,
Kurpińskiego 5,
85-950 Bydgoszcz, Poland
e-mail: robert.zalesny@cm.umk.pl

K. Matczyszyn · W. Bartkowiak
Institute of Physical and Theoretical Chemistry,
Wrocław University of Technology,
Wyb. Wyspiańskiego 27,
50-370 Wrocław, Poland

A. Kaczmarek
Research Group for Modeling and Synthesis of Novel Materials,
Faculty of Chemistry, Nicolaus Copernicus University,
Gagarina 7,
87-100 Toruń, Poland

Introduction

Azobenzenes are a group of molecules extensively studied both experimentally [1–15] as well as theoretically [14–22]. The interest in this class of compounds is mainly due to the photoswitching between *cis* and *trans* conformers and applicability in the field of photonics. Polymeric matrices with photoactive azobenzenes can be used as surface relief gratings [23], molecular switches or all-optical memories [7], just to mention only a few of the possible applications. Azobenzene molecule is known to undergo a photoisomerization from *trans* to *cis* conformation upon irradiation by light. The reverse transformation (from *cis* to *trans* conformer) occurs either thermally or upon irradiation by light. It is well recognized that substituents can strongly affect the barrier to *trans–cis* isomerization [3, 21]. Additionally, the rate of the process and the barrier to isomerization depend on the environment (solvent, polymer matrix, liquid crystal, etc.) [3, 11]. On the other hand, the polarity of the environment may induce substantial changes of dipole moment, polarizability and first-order hyperpolarizability of azobenzene derivatives.

The calculation of electronic spectra of large molecules is a challenging problem. Simultaneously, most of the advanced methods of the electronic structure theory which can be used for accurate calculations of the electronic spectra of large molecules are very demanding computationally. This can be taken as a rationale for the use of highly simplified approaches which permit inexpensive calculations for large molecules. Among these methods, the configuration interaction approach with single excitations only (CIS) and time-dependent density functional theory (TDDFT) have become one of the most frequently used [24]. The CIS method is known to give too high or much too high excitation energies. A significant improvement can be gained by using correc-

tions evaluated in the spirit of perturbation methods for multideterminantal wave functions [25]. This, however, considerably increases the computing time.

The aim of the present study is twofold. Firstly, we analyze different methods of calculations of electronic excitations of series of polymethylmethacrylate (PMMA) copolymers with attached azobenzene derivatives by comparing the results with experimental data. Secondly, we present the results of calculations of the electric dipole moments and analyze the nature of the experimentally observed excitations.

Experimental methods

The series of polymethylmethacrylate (PMMA) copolymers with azobenzene derivatives was synthesized by Paul Raimond (Commissariat a l'Energie Atomique, Saclay, France). The four investigated copolymers were dissolved in 1,1,2-trichloroethane (Merck, spectroscopic grade). The molar concentration of the solutions was 10^{-4} M. The UV-Vis spectra were measured with the Perkin Elmer Lambda 20 spectrophotometer equipped with the Peltier thermostat and the external source of light. The samples were irradiated

Fig. 1 Schematic representation of investigated PMMA copolymers with azobenzene derivatives
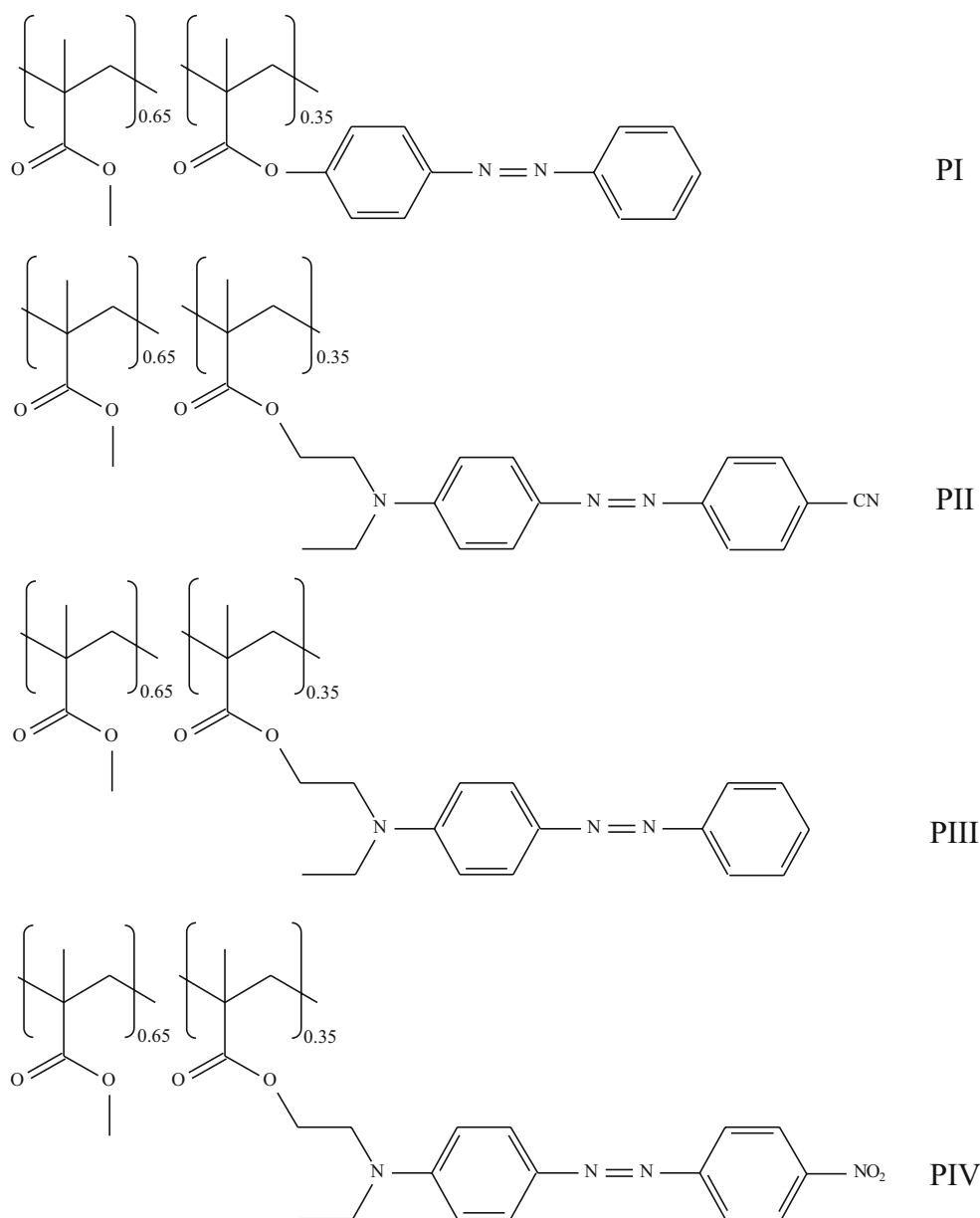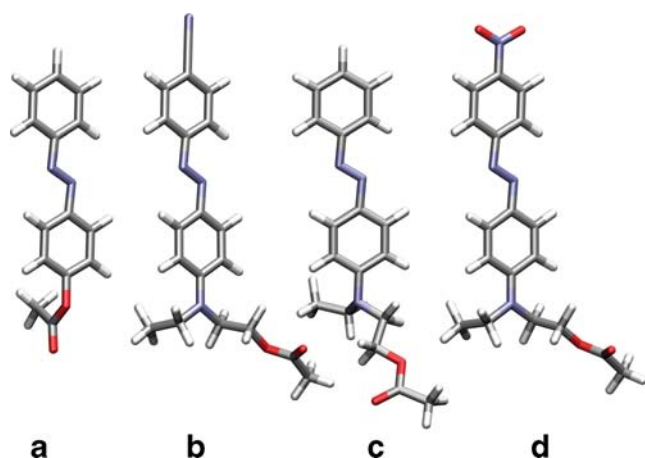
Fig. 2 Geometrical structure of azobenzene derivatives optimized in tetrahydrofuran at the B3LYP/6-311++G(d,p) level of theory. **a** Acetic acid 4-phenylazo-phenyl ester; **b** acetic acid 2-([4-(4-cyanophenylazo)-phenyl]ethyl-amino)-ethyl ester; **c** acetic acid 2 [ethyl (4-phenylazo-phenyl)-amino]ethyl ester; **d** acetic acid 2-(ethyl[4-(4-nitro-phenylazo)-phenyl]-amino)-ethyl ester

with the use of mercury lamp (200W Hg, high pressure) and the combination of appropriate interference filters (UV power $I_0 = 1.15 \cdot 10^{-3}$ W/m^2, VIS power $I_0 = 7,0 \cdot 10^{-6}$ W/m^2).

Computational details

All quantum-chemical calculations were performed using the Gaussian 03 suite of programs [26]. The geometrical parameters of investigated molecules were optimized at the B3LYP/6-311++G(d,p) level of theory. All stationary points were confirmed to be minima by the evaluation of Hessian. The solvent effects were included during geometry optimizations using IEF-PCM method [27–29]. The IEF (integral equation formalism) version of the PCM solvation model was proved to be robust and effective [28]. Excitation energies were calculated using TDDFT [30, 31] with the 6-311++G(d,p) basis set and two functionals, namely B3LYP and PBE0. Similarly to the geometry optimizations, in the TDDFT calculations the solvent effects were taken into account via the IEF-PCM method. The analysis of the character of the transitions in terms of occupied and virtual molecular orbitals was performed using the transition vectors as the solutions of the finite dimensional time-dependent Kohn-Sham eigenvalue problem [32–34].

Additionally, excitation energies were computed using the CIS method. The CIS calculations were performed using the direct algorithm. Unfortunately, the current implementation of the CIS(D) method in the Gaussian 03 program does not allow for inclusion of the solvent effects.

Hence, the results of CIS(D) excitation energies are not presented in this paper.

In order to estimate the polarity of the excited states, the dipole moment differences between ground and excited states were calculated by numerical differentiation of the excitation energies:

$$\Delta\mu_{ge}^i = \frac{\Delta E(+F^i) - \Delta E(-F^i)}{2F^i}$$

where g and e are indices standing for the ground and excited state, respectively. The index i denotes the Cartesian component of the dipole moment difference. The electric field F of strength 0.001 au was used in all calculations. The numerical stability of $\Delta\mu$ calculations was checked by comparing analytical dipole moments from the ground state calculations with the values obtained by numerical differentiation of the ground state energy.

The contour surfaces of molecular orbitals were plotted using Molden program [35].

Results and discussion

The chemical structure of four polymethylmethacrylate (PMMA) copolymers with attached azobenzene derivatives (**PI–PIV**) are presented in Fig. 1. These copolymers were dissolved in 1,1,2-trichloroethane. In Fig. 2, we present the azobenzene derivatives that mimic PMMA copolymers used in all subsequent calculations of excitation energies and dipole moments, both in the ground as well as excited states. In our opinion, it is not necessary to include more polymer units in simulation of Vis spectra, because the excitations in this spectral range occur in the side chain (azobenzene moiety). The geometries of azobenzenes
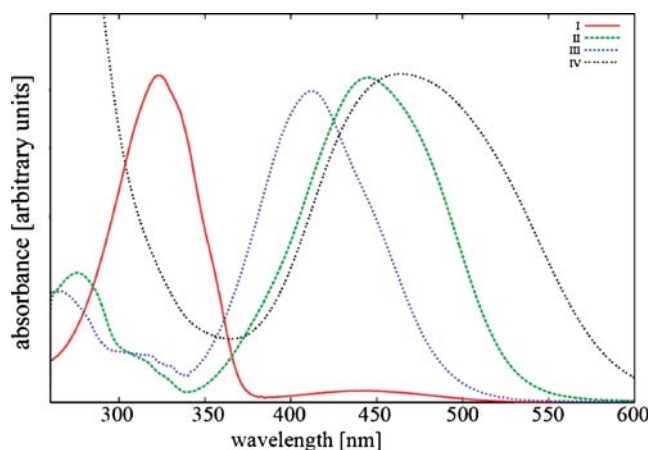

Fig. 3 UV-Vis spectra of investigated PMMA copolymers with azobenzene derivatives dissolved in 1,1,2-trichloroethane

Table 1 The UV-Vis excitation energies (ΔE) and oscillator strengths (f) for the model molecules calculated at the TDDFT/6-311++G(d,p) level of theory with the inclusion of the solvent effects by the IEF-PCM model

Model molecules	ΔE and f values		
	S_1	S_2	S_3
I			
B3LYP	ΔE=482 nm; f=0.000 (n→π*)	ΔE=357 nm; f=0.998 (π→π*)	ΔE=316 nm; f=0.034 (π→π*)
PBE0	ΔE=479 nm; f=0.000 (n→π*)	ΔE=346 nm; f=1.026 (π→π*)	ΔE=304 nm; f=0.033 (π→π*)
CIS (Exp.)	(440 nm)	279 nm (321 nm)	
II			
B3LYP	ΔE=489 nm; f=0.002 (n→π*)	ΔE=461 nm; f=1.334 (π→π*)	ΔE=314 nm; f=0.023 (π→π*)
PBE0	ΔE=483 nm; f=0.001 (n→π*)	ΔE=447 nm; f=1.375 (π→π*)	ΔE=302 nm; f=0.013 (π→π*)
CIS (Exp.)		330 nm (441 nm)	
III			
B3LYP	ΔE=479 nm; f=0.000 (n→π*)	ΔE=411 nm; f=0.656 (π→π*)	ΔE=331 nm; f=0.036 (π→π*)
PBE0	ΔE=475 nm; f=0.000 (n→π*)	ΔE=393 nm; f=0.736 (π→π*)	ΔE=318 nm; f=0.362 (π→π*)
CIS (Exp.)		287 nm (412 nm)	
IV			
B3LYP	ΔE=535 nm; f=1.070 (n→π*)	ΔE=523 nm; f=0.002 (n→π*)	ΔE=377 nm; f=0.343 (π→π*)
PBE0	ΔE=507 nm; f=0.116 (n→π*)	ΔE=504 nm; f=1.068 (π→π*)	ΔE=356 nm; f=0.251 (π→π*)
CIS (Exp.)		314 nm (470 nm)	

The values from CIS/6-311++G(d,p) calculations are in the last row for a given molecule. The numbers in parentheses are experimental absorption band maxima.

presented in Fig. 2 were obtained at the B3LYP/6-311++G (d,p) level of theory with the inclusion of solvent effects (see Computational details). However, in all calculations, instead of 1,1,2-trichloroethane we used tetrahydrofuran (THF). Both 1,1,2-trichloroethane and THF have virtually the same dielectric constant, but the former is not parametrized in the current implementation of the PCM method in the Gaussian program. Nevertheless, during the geometry optimization and calculations of electronic spectra only electrostatic contributions were included.
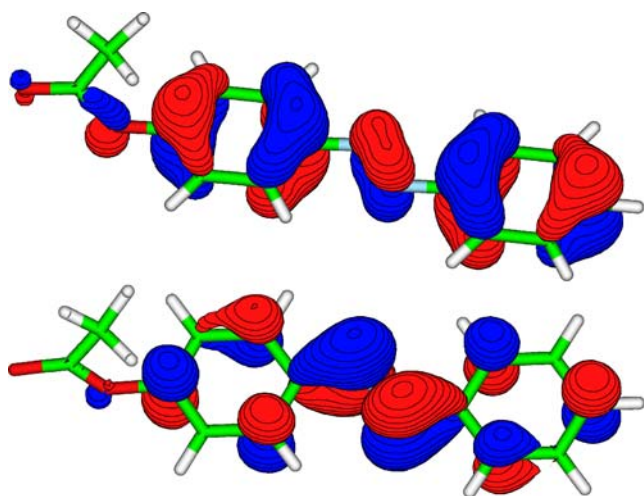
In Fig. 3, we present the recorded spectra of four investigated PMMA copolymers substituted with azobenzenes and dissolved in 1,1,2-trichloroethane. Similarly to the unsubstituted azobenzene molecule, all PMMA copolymers investigated here exhibit a very intense absorption band associated with π→π* transition. In the case of unsubstituted azobenzene molecule, the peak of this band is located near 330 nm in heptane [10]. Values of experimental absorption band maxima for π→π* transitions are presented in Table 1.

Fig. 4 The plots of orbital contour surfaces for molecule **I**. The molecular orbitals were calculated at the PBE0/6-311++G(d,p) level of theory. The *upper plot* presents contour surface of HOMO and the *lower* presents contour surface of LUMO. Shown are the contour surfaces of orbital amplitude 0.04 (*red*) and −0.04 (*blue*)

Fig. 5 The plots of orbital contour surfaces for molecule **II**. The molecular orbitals were calculated at the PBE0/6-311++G(d,p) level of theory. The *upper plot* presents contour surface of HOMO and the *lower* presents contour surface of LUMO. Shown are the contour surfaces of orbital amplitude 0.04 (*red*) and −0.04 (*blue*)
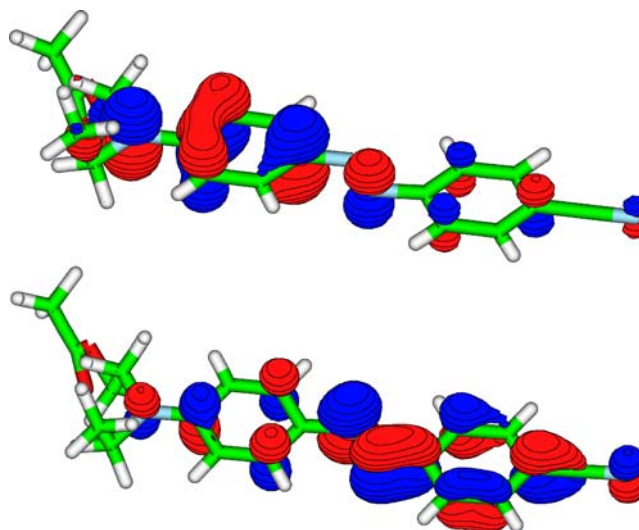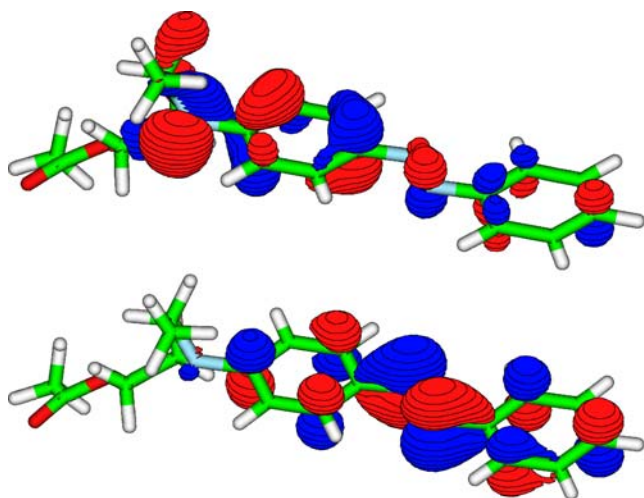
Fig. 6 The plots of orbital contour surfaces for molecule **III**. The molecular orbitals were calculated at the PBE0/6-311++G(d,p) level of theory. The *upper plot* presents contour surface of HOMO and the *lower* presents contour surface of LUMO. Shown are the contour surfaces of orbital amplitude 0.04 (*red*) and −0.04 (*blue*)

For **I**, **II**, **III** and **IV**, the band maxima are located at 321 nm, 441 nm, 412 nm and 470 nm, respectively. For molecule **I**, the recorded spectra also reveals a much weaker band with the maximum located near 440 nm. This band is associated with the n→π* transition.

In Table 1, we compare the theoretically determined excitation energies of π→π* transition with the experimental values and present the results obtained using TDDFT method with B3LYP and PBE0 functionals as well as CIS method. As expected, the CIS method overestimates excitation energy of the π→π* transition for all studied azobenzene derivatives. The differences between the experimental band maxima and the CIS values range from 42 nm for molecule **I** to 156 nm for molecule **IV**. Since the CIS results are of a qualitative character, we included values in Table 1 for the second singlet state $S_2(\pi, \pi^*)$ only. Recent papers of Perpète et al. [36] and Jacquemin et al. [37–39] have shown that the parameter-free PBE0 functional combined with appropriate basis set can provide very accurate excitation energies. This observation is consistent with the results obtained in the present study. The differences between the experimental band maxima for the $S_2(\pi, \pi^*)$ state and the PBE0 excitation energies for molecules **I**, **II**, **III** and **IV** are −25 nm, −6 nm, 19 nm and −34 nm, respectively. For comparison, the respective differences for the B3LYP method are −36 nm, −20 nm, 1 nm and −53 nm for molecules **I**, **II**, **III** and **IV**, respectively. It is evident that the PBE0 excitation energies are more accurate than the B3LYP values. For this reason, the frontier orbitals analysis of the nature of excitations is performed using the PBE0 method.

Values of excitation energies of lowest singlet states, i.e. $S_1(n, \pi^*)$ and $S_3(\pi, \pi^*)$ are also included in Table 1. As was mentioned before, the n→π* transition is visible in the

recorded spectra only for molecule **I**. The difference between PBE0 excitation energy and the band maximum associated with the n→π* transition is quite large, i.e. 39 nm. Assuming that the PBE0 values of excitation energies to the S (n, π*) states for other molecules are at least semi-quantitative, one can conclude that, in the case of molecules **II**, **III** and **IV**, the weak, symmetry-forbidden n→π* transitions are overlapped by the band arising from the very intense π→π* transition.

In order to gain some insight into the nature of the $S_2(\pi, \pi^*)$ excited states for investigated azobenzene derivatives, we performed the analysis in the spirit of the single excited configurations. In the case of all studied molecules, we found that the π→π* transition is dominated by the HOMO→LUMO transition. The expansion coefficients for this configuration, at the PBE0/6-311++G(d,p) level of theory, were 0.65, 0.64, 0.67 and 0.62 for molecules **I**, **II**, **III** and **IV**, respectively. The plots of the HOMO and LUMO contour surfaces for all four molecules are presented in Figs. 4, 5, 6 and 7. The assignments of the transitions presented in Table 1 were performed based on the analysis of LCAO MO coefficients. The plots presented in Figs. 4, 5, 6 and 7 confirm these assignments. For all investigated molecules, the excitation involves π–bonding and π*-antibonding orbitals of nitrogen atoms in the azobenzene moiety. It is interesting to compare the change of contour surfaces upon excitations (Figs. 4, 5, 6 and 7) with the calculated dipole moment differences presented in
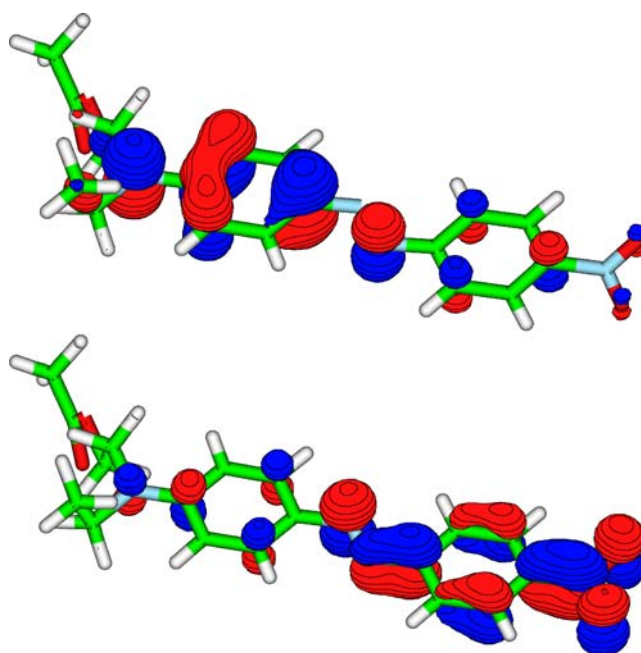

Fig. 7 The plots of orbital contour surfaces for molecule **IV**. The molecular orbitals were calculated at the PBE0/6-311++G(d,p) level of theory. The *upper plot* presents contour surface of HOMO and the *lower* presents contour surface of LUMO. Shown are the contour surfaces of orbital amplitude 0.04 (*red*) and −0.04 (*blue*)

Table 2 The dipole moments for the model molecules calculated using the 6-311++G(d,p) basis set with the inclusion of the solvent effects by the IEF-PCM model. Indices g and e denote the ground and the lowest excited (π,π^*) state, respectively

Form (state)	$\mu_g^z(\mu)$ [au]				$\Delta\mu_{ge}^z$ [au]	
	B3LYP		PBE0		B3LYP	PBE0
I	5.59	(6.21)	5.55	(6.17)	−0.13	−0.12
II	−13.27	(14.19)	−13.10	(14.01)	−3.36	−3.51
III	0.63	(2.93)	0.64	(2.95)	−5.40	−5.10
IV	−15.09	(15.92)	−14.69	(15.51)	−5.04	−4.07

$\Delta\mu_{ge}^z$ stands for the dipole moment difference bewteen the ground and the lowest excited (π,π^*) state. The values of the total dipole moments in the ground state are given in parentheses.

Table 2. The longitudinal dipole moment components in the S_0 state are 5.55, −13.10, 0.64 and −14.69 au for molecules **I**, **II**, **III** and **IV**, respectively (results from PBE0 calculations). These values agree with the chemical intuition: the largest dipole moment is for molecule **IV** with very strong acceptor group ($-NO_2$) and the smallest μ_g^z value for molecule **III**. Since molecule **II** is substituted with the weaker acceptor group ($-CN$) than molecule **I**, the smaller value of the ground state dipole moment for **I** than for **II** is to be expected. This difference based on PBE0/6-311++G(d,p) calculations is 1.50 au for the total dipole moment and 1.59 au for the longitudinal component of the dipole moment. What concerns the $S_2(\pi,\pi^*)$ state is that in the cases of all molecules we found the change of the longitudinal component of the dipole moment. With the exception of molecule **I**, the $S_2(\pi,\pi^*)$ state is of significantly different polarity than the ground state. The largest change of μ_g^z is observed for molecule **III**. Hence, strong dependence of the absorption band maxima on the solvent polarity is expected for molecules **II**, **III** and **IV**. More accurate results of dipole moment differences between the ground and the charge transfer states could be obtained using Coulomb-attenuated density-functional theory [40].

observed large values of $\Delta\mu_{ge}^z$ of these molecules make them attractive objects for various nonlinear optical applications.

Conclusions

In the present study, we reported on the comparison of the experimental and the theoretical calculations of excitation energies for substitued azobenzenes. Although the primary goal of the present study was to analyze the recorded spectra and the observed excitations, we found that the PBE0 functional with 6-311++G(d,p) basis set satisfactorily reproduces the experimental data. The B3LYP functional was less accurate but it gave reliable results. As expected, the CIS method gave too high excitation energies. It was found that, in three cases (molecules **II**, **III** and **IV**), the experimentally observed strong absorption bands correspond to the transitions to the singlet state $S_2(\pi,\pi^*)$ of significantly different polarity than the ground state (more than 8 D). The

References

1. Schanze KS, Mattox TF, Whitten DG (1982) J Am Chem Soc 104:1733–1735
2. Schanze KS, Mattox TF, Whitten DG (1983) J Org Chem 48:2808–2813
3. Nishimura N, Kosako S, Sueishi Y (1984) Bull Chem Soc Jpn 57:1617–1625
4. Sueishi Y, Asano M, Yamamoto S, Nishimura N (1985) Bull Chem Soc Jpn 58:2729–2730
5. Sugihara O, Kunioka S, Nonaka Y, Aizawa R, Koike Y, Kinoshita T, Sasaki K (1991) J Appl Phys 70:7249–7252
6. Harada J, Ogawa K, Tomoda S (1997) Acta Cryst B 53:662–672
7. Kawata S, Kawata Y (2000) Chem Rev 100:1777–1788
8. Ichimura K (2000) Chem Rev 100:1847–1873
9. Tamai N, Miyasaka H (2000) Chem Rev 100:1875–1890
10. Matczyszyn K, Bartkowiak W, Leszczynski J (2001) J Mol Struct 565–566:53–57
11. Matczyszyn K, Sworakowski J (2003) J Phys Chem B 107:6039–6045
12. Schmidt B, Sobotta C, Malkmus S, Laimgruber S, Braun M, Zinth W, Gilch P (2004) J Phys Chem A 108:4399–4404
13. Blevins AA, Blanchard GJ (2004) J Phys Chem B 108:4962–4968
14. Poprawa-Smoluch M, Baggerman J, Zhang H, Maas HPA, De Cola L, Brouwer AM (2006) J Phys Chem A ASAP publication
15. Kucharski S, Janik R, Motschmann H, Radüge C (1999) New J Chem 23:765–771
16. Cimiraglia R, Hofmann HJ (1994) Chem Phys Lett 217:430–435
17. Cimiraglia R, Asano T, Hofmann HJ (1996) Gaz Chim Ital 126:679–684
18. Cattaneo P, Persico M (1999) Phys Chem Chem Phys 1:4739–4743
19. Tamulis A, Tamuliene J, Balevicius ML, Nunzi JM (2000) Mol Cryst Liq Cryst 354:1063–1072
20. Diau EWG (2004) J Phys Chem A 108:950–956
21. Crecca CR, Roitberg AE (2006) J Chem Phys A 110:8188–8203
22. Nonnenberg C, Gaub H, Frank I (2006) Chem Phys Chem 7:1455–1461
23. Lagugnè-Labarthet F, Adamietz F, Rodriguez V, Sourisseau C (2006) J Phys Chem B 110:13689–13693

24. Dreuw A, Head-Gordon M (2005) Chem Rev 105:4009–4037
25. Head-Gordon M, Rico RJ, Oumi M, Lee TJ (1994) Chem Phys Lett 219:21–29
26. Gaussian 03, Revision C.02, Frisch MJ, Trucks GW, Schlegel HB, Scuseria GE, Robb MA, Cheeseman JR, Montgomery Jr JA, Vreven T, Kudin KN, Burant JC, Millam JM, Iyengar SS, Tomasi J, Barone V, Mennucci B, Cossi M, Scalmani G, Rega N, Petersson GA, Nakatsuji H, Hada M, Ehara M, Toyota K, Fukuda R, Hasegawa J, Ishida M, Nakajima T, Honda Y, Kitao O, Nakai H, Klene M, Li X, Knox JE, Hratchian HP, Cross JB, Bakken V, Adamo C, Jaramillo J, Gomperts R, Stratmann RE, Yazyev O, Austin AJ, Cammi R, Pomelli C, Ochterski JW, Ayala PY, Morokuma K, Voth GA, Salvador P, Dannenberg JJ, Zakrzewski VG, Dapprich S, Daniels AD, Strain MC, Farkas O, Malick DK, Rabuck AD, Raghavachari K, Foresman JB, Ortiz JV, Cui Q, Baboul AG, Clifford S, Cioslowski J, Stefanov BB, Liu G, Liashenko A, Piskorz P, Komaromi I, Martin RL, Fox DJ, Keith T, Al-Laham MA, Peng CY, Nanayakkara A, Challacombe M, Gill PMW, Johnson B, Chen W, Wong MW, Gonzalez C, Pople JA, Gaussian, Wallingford CT, 2004
27. Cancès E, Mennucci B, Tomasi J (1997) J Chem Phys 107:3032–3040
28. Tomasi J, Mennucci B, Cancès E (1999) J Mol Str (Theochem) 464:211–226
29. Chipman DM (2002) Theor Chem Acc 107:80–89
30. Marques MAL, Gross EKU (2004) Annu Rev Phys Chem 55:427–455
31. Furche F, Burke K (2005) Time-dependent density functional theory in quantum chemistry. In: Spellmeyer D (ed) Annual Reports in Computational Chemistry, Vol 1. Elsevier
32. Casida ME (1995) Time-dependent density functional response theory for molecules. In: Chong DP (ed) Recent advances in density functional methods. World Scientific, Singapore
33. Van Leeuwen R (2001) Int J Mod Phys B 15:1969–2023
34. Appel H, Gross EKU, Burke K (2003) Phys Rev Lett 90:043005
35. Schaftenaar G, Noordik JH (2000) J Comp Aided Mol Des 14:123–134
36. Perpète EA, Wathelet V, Preat J, Lambert C, Jacquemin D (2006) J Chem Theory Comput 2:434–440
37. Jacquemin D, Bouhy D, Perpète EA (2006) J Chem Phys 124:204321
38. Jacquemin D, Wathelet V, Perpète EA (2006) J Phys Chem A 110:9145–9152
39. Jacquemin D, Preat J, Wathelet V, Fontaine M, Perpète EA (2006) J Am Chem Soc 128:2072–2083
40. Ruudberg E, Salek P, Helgaker T, Ågren H (2005) J Chem Phys 123:184108